J. Min. Metall. Sect. B-Metall. 53 (1) B (2017) 75 - 81

Journal of Mining and Metallurgy,
Section B: Metallurgy

MELT QUALITY INDUCED FAILURE OF ELECTRICAL CONDUCTOR (EC) GRADE ALUMINUM WIRES

A. Khaliq[a,b], M.A. Rafiq[b], H.T. Ali[c], F. Ahmed[b], S. Mehmood[d], J. Grandfield[e], S.A. Ranjha[a]

[a]Faculty of Science, Engineering and Technology, Swinburne University of Technology, Melbourne, Australia
[b]Metallurgical and Materials Engineering Department, University of Engineering and Technology, Lahore, Pakistan
[c]Advanced Composites Centre for Innovation and Science (ACCIS), Department of Aerospace Engineering, University of Bristol, Bristol, UK
[d]Northern Ireland Advanced Composites & Engineering Centre, Belfast, UK
[e]Grandfield Technologies Pty Limited, Coburg, Victoria, Australia

(Received 06 October 2015; accepted 24 November 2016)

Abstract

The failure of electrical conductor grade (EC) aluminum during wire drawing process was investigated. The fractured aluminum wires were subjected to Scanning Electron Microscopy (SEM) and Energy Dispersive X-ray (EDX) analyses for an initial examination. Thermodynamic analyses of molten aluminum interaction with refractories was also carried out using FactSage at 710 ^oC to predict the stable phases. The SEM/EDX analyses has revealed the inclusions in aluminum matrix. The typical inclusions observed were Al_2O_3, Al_3C_4 (Al-Carbide) and oxides of refractories elements (Al, Mg, Si and O) that have particle size ranging up to 5 µm. The transition metal boride particles were not identified during SEM/EDX analyses these might be too fine to be detected with this microscope. The overall investigation suggested that the possible cause of this failure is second phase particles presence as inclusions in the aluminum matrix, and this was associated with the poor quality of melt. During wire drawing process, these inclusions were pulled out of the aluminum matrix by the wire-drawing forces to produce micro-voids which led to ductile tearing and final fracture of wires. It was recommended to use ceramic foam filters to segregate inclusions from molten aluminum.

Keywords: *Aluminum wire drawing; Inclusions; Ductile fracture; Scanning electron microscope (SEM), Oxides and carbides*

1. Introduction

The presence of transition metals in the melt reduces the electrical conductivity of smelter grade aluminum [1, 2]. Boron treatment has widely been used for the removal of Ti, V and Zr from an aluminum melt in the form of their stable borides [3-10]. During boron treatment of molten aluminum, Al-B master alloys (AlB_2/AlB_{12}) are used in the form of waffles, rods or wires depending on the melting practice and end product requirements. Once Al-B master alloy is introduced, electrical conductivity of melt increased in the first couple of minutes [3-6, 11-14]. Khaliq *et. al* [14] have reported the formation of borides placed in shell around initially added particles of AlB_2/AlB_{12} in the aluminum matrix. SEM and EDX analyses of Al-1wt%V-0.412wt%B system suggested the presence of V, B and Al in the outer shells, formed during the solidification of samples or boron treatment process. It was further proposed that the dissolution of AlB_{12} particles was sluggish as they were partially dissolved even after one hour of melt holding in the induction stirring [15]. The boride inclusions generated during boron treatment are thermodynamically stable hence these don't dissolve during holding of the molten aluminum for 6 to 12 hours at 725^{o}C [13, 14, 16, 17]. The size of boride inclusions could be more than 100 µm, as shown in Figure 1. Predominantly, larger boride particles settled at the bottom of holding furnace in the first 3 to 4 hours of boron treatment process [14].

Comparatively, longer holding time is practiced to settle smaller (< 10µm) inclusions from molten aluminum. This results in low productively and higher cost for boron treatment of the molten aluminum. Therefore, ceramic form filters are employed to trap the smaller inclusions generated during melt treatment in the cast house [18, 19].

The quality of end product depends on the level of inclusions and cleanliness of the melt. It is essential to control level of undesirable impurities to ensure better performance of aluminum during service. The sources

* *Corresponding author: aks1445@gmail.com*

DOI:10.2298/JMMB151006030K

of impurities in aluminum (produced by Hall-Heroult process) are raw materials (bauxite and petroleum coke), cell materials (carbon cathodes, linings) and others (furnaces, ladles and launders linings) which come in contact with melt during different stages of refining processes in the cast house [20]. A list of common inclusions and impurities found in aluminum is presented in Table 1. Impurities in a downstream product may be present in the form of dissolved elements, oxides, borides, nitrides, chlorides, silicates and fluorides as summarized in Table 1. Each form of these impurities can cause problems and can lead to die failure during high pressure die casting and wire drawing processes. Impurities are also a source of porosity and pinholes in the thin sheets of aluminum [21].

Generally, 1000 series aluminum alloys are employed as an electrical conductor due to better electrical conductivity. For instance, 1350 series alloys have 99.50wt% aluminum and possess electrical conductivity of 61 to 62 % International Annealed Copper Standard (IACS) [25]. Others aluminum alloys including 6000 series are widely used for long distance power transmission. These conductors are reinforced with galvanized steel or Invar (Fe-Ni alloys) to increase load bearing capacity of composite cables that are known as aluminum alloy conductor steel reinforced (ACSR). Such composite cables are composed of aluminum alloy wires in the outer layers and steel rods in the core [25-27]. A schematic configuration of ACSR has been reported in [28, 29]. For better mechanical strength, certain alloying ingredients such as Zr are added in the aluminum conductors. However, such alloying additions have detrimental effect on the electrical conductivity of 1000 series aluminum alloys [26, 30]. Erturk *et al*. (2015) [26] have investigated the manufacturing of Al-Zr heat resistant alloys for overhead power transmissions lines. These alloys have a capability to maintain mechanical strength at much higher temperatures i.e. 150 ^{o}C to 200 ^{o}C compared to 75 ^{o}C that is suitable for ordinary electrical conductor materials. The formation and dispersion of Al_3Zr particles limit the recrystallization process at higher temperatures hence mechanical properties are improved for Al-Zr alloys.

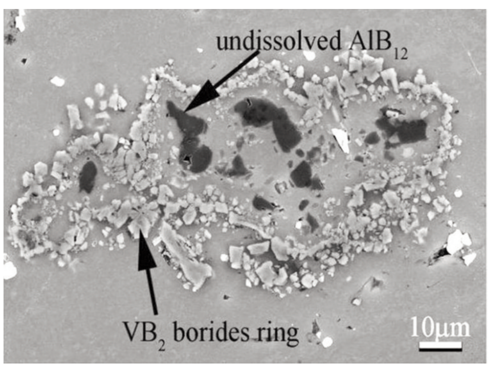

Figure 1. *SEM image of Al-B (AlB_{12}) and VB_2 particles in the Al-V-B alloys at 750^{o}C [12]*

Electrical conductors (EC) and ACSR are manufactured through continuous casting lines (CCL) technology in industry [6, 7]. Continuous casting lines are composed of melting and holding furnaces, casting wheels, and rolling machines. The schematic of the whole assembly is given in [6]. The processing routes of extrusion, rolling, wire drawing and stranding are also employed for the manufacturing of electrical conductor cables, bus shapes and tubes [25]. Aluminum melt quality and inclusions play critical role, especially, during the process of wire drawing where feedstock diameter is reduced to less than 10 *mm*. The incoherency of inclusions with aluminum matrix leads to the generation of weaken regimes that generally trigger the fracture of cables during wire drawing processes. Therefore, it is essential to investigate the generation of inclusions during melting and holding of aluminum alloys in the cast house.

This study is dedicated to the generation of inclusions in molten aluminum and the failure of electrical conductor grade aluminum wires. For this, thermodynamic and experimental analyses of molten aluminum interaction with refractory materials was

Table 1. *Inclusions and impurities in aluminum [20-24]*

Dissolved Impurities			Solid Inclusions	
Metals		Gases	Refractory - Electrolysis	
Primary	*Re-melted*		*Exogenous*	*Endogenous*
Sodium	Iron	Hydrogen	Al_2O_3,MgO (10–1000 μm)	Al_4C_3 (0.5–25μm)
Lithium	Silicon		Al_2O_3.MgO (50-500 μm)	
Calcium	Manganese		K,Ca,Al-Silicates (10-100 μm)	
Magnesium	Copper		Na,Ca,Mg Aluminates (50-500 μm)	
Vanadium			Borides	
Nickel			Nitrides	
Zirconium				

carried out at 710°C. Scanning electron microscope (SEM) was used to investigate the failure of aluminum wires. while the chemical composition of the observed phases were estimated with energy dispersive X-ray (EDX) analysis. Section I outlines problem statement and Section II describes the thermodynamics analysis of the interaction between refractory materials and molten aluminum, and the generation of inclusions. The experiments and their results are presented in Sections III and IV respectively. Some of the key findings are highlighted in Section V of this manuscript.

2. Thermodynamic Analysis of Inclusions Generation in Molten Aluminum

Firstly, the interaction of commonly used refractories with molten aluminum was investigated using FactSage, a thermodynamic package. For this, three types of refractory materials commonly used in the cast houses were selected. These refractories come in contact with molten aluminum at various stages of melting and casting processes in the cast house. For instance, refractory material (A) is used to transfer molten aluminum to direct chilled casting molds. However, refractory materials (B) is used for the patching of damaged section of the launders that transfer molten aluminum to the continuous casting lines (CCL). The chemical compositions of the refractory materials are presented in Table 2.

Table 2. *Refractory materials and their chemical compositions*

Chemical Composition (wt%)	Refractory Materials		
	A	B	C
SiO_2	60	48-58	79.7
Al_2O_3	29	42-52	16.5
CaO	11	-	1.6
TiO_2	-	-	0.4
Fe_2O_3	-	-	0.3
Others	-	-	1.5

Equilibrium calculations were carried out at 710°C that is a temperature maintained during boron treatment of the molten aluminum. The "Equilib" module that incorporates the Gibbs free energy minimization criteria was used. During these calculations FactPS, and FT Oxide databases were used. For each calculation, a mass of 1000 grams Al and 50 grams of refractories (A, B & C) were used in the input data as shown in Table 2. The list of predicted phases during interaction between molten aluminum and refractories are summarized in Table 3. Thermodynamic analysis predicted that Ca-aluminates such as $CaAl_4O_{7(s)}$ and $CaAl_{12}O_{19(s)}$ are stable solid phases in the presence of Ca in refractory materials. However, in the absence of Ca, only $Al_2O_{3(s)}$ would be stable phase in the molten aluminum. From this analyses, it may be possible to trace the origin of inclusions in the downstream products. Individual Al_2O_3 particles could be originated from the reduction of SiO_2 in the refractories.

Table 3. *The predicted phases during interaction of refractories and molten aluminum at 710°C*

Ref. Mat.	Elements/Oxides in the final product					
A	$Al_{(liq)}$	$CaAl_4O_{7(s)}$	$CaAl_{12}O_{19(s)}$	$Si_{(s)}$	-	-
B	$Al_{(liq)}$	$Al_2O_{3(s)}$	$Si_{(s)}$	-	-	-
C	$Al_{(liq)}$	$Al_2O_{3(s)}$	$CaAl_{12}O_{19(s)}$	$Si_{(s)}$	$Si_2Ti_{(s)}$	$FeAl_{3(s)}$

Contrary to this, the present of Ca in the inclusion may come from refractories containing Ca (materials A and C). It is worth noting that the analysis is purely based on the thermodynamic calculations and does not incorporate the kinetic parameters.

It is concluded from the thermodynamic analysis that inclusions including Al_2O_3 and Ca-aluminates may be generated during the interaction of molten aluminum and refractories. These inclusions may contribute to the failure of downstream products such as wires, sheets and foils made from molten aluminum.

3. Experimental Approach

Smelter grade aluminum ingots were obtained from one of the smelters in Australasia. The composition of the smelter grade aluminum has been reported in [31]. The boron treatment of molten aluminum was carried out in 5 tons melting and holding furnace in the cast house. The Al-B master alloys used for boron treatment were obtained from London and Scandinavian Metallurgical Co (LMS) presently a part of AMG super alloys UK. The predominant phase in the Al-10wt%B master alloy was AlB_{12}. Aluminum ingots were melted in the gas fired furnace and a temperature of 720±10 °C was maintained. The addition of Al-10wt%B (AlB_{12}) master alloy was 200wt% in excess to the stoichiometric requirement of the transition metal removal assuming their di-borides formation in the molten aluminum. The stirring of the molten pool of aluminum was conducted with a long paddle for 2 to 3 minutes. Dross was removed from the surface and molten aluminum was held for 3-4 hours for the settling of borides and other associated impurities. Finally, electrical conductor grade (EC) aluminum rods were produced in a continuous casting lines

CC BY SA

(CCL) and subsequent wire drawing to various diameters. A similar set-up for the melting and holding furnace was reported earlier in [14]. The failure of aluminum wires as observed during wire drawing process is shown in Figure 2.

Figure 2. *Digital image of fractured EC grade aluminum wire after wire drawing die assembly*

4. Investigation Methodology
4.1 Fractured Surface Analysis

The fractured ends and surfaces of the EC-grade aluminum wires were investigated using SUPRA 40VP-25-38 SEM, without causing any damage to them. The purpose of this analysis was to locate any possible second phase particles or inclusions in the aluminum matrix to verify the cause of wires failure. Figures 3, 4, 7 and 8 show secondary electron images taken from the fractured surface of the aluminum wire. Some rippled surfaces and chevron cracks have also been observed in Figures 3c. The phenomenon of cracking and inclusions existence have been observed in the Figures 4a and 4b. Micro cracks on the surface of the wires were observed under high resolutions which contain other phases inside these openings. The broken end of aluminum wire is shown in Figures 4c. It is obvious from these observations that some material has been removed from aluminum matrix, leaving behind a cavity in the broken end. It might be the inclusion/or clusters of inclusions removal which did not develop high strength bond with aluminum matrix.

4.2 EDX Analysis
4.2.1 Point Analysis

The point's analyses of various samples obtained by EDX are shown in Figure 5. The point analysis of inclusions at various locations revealed the presence of Al, O, C and Mg in the aluminum matrix. The presence of Al and O are in accordance with the thermodynamic predictions as discussed in Section II. This confirmed the presence of alumina (Al_2O_3)

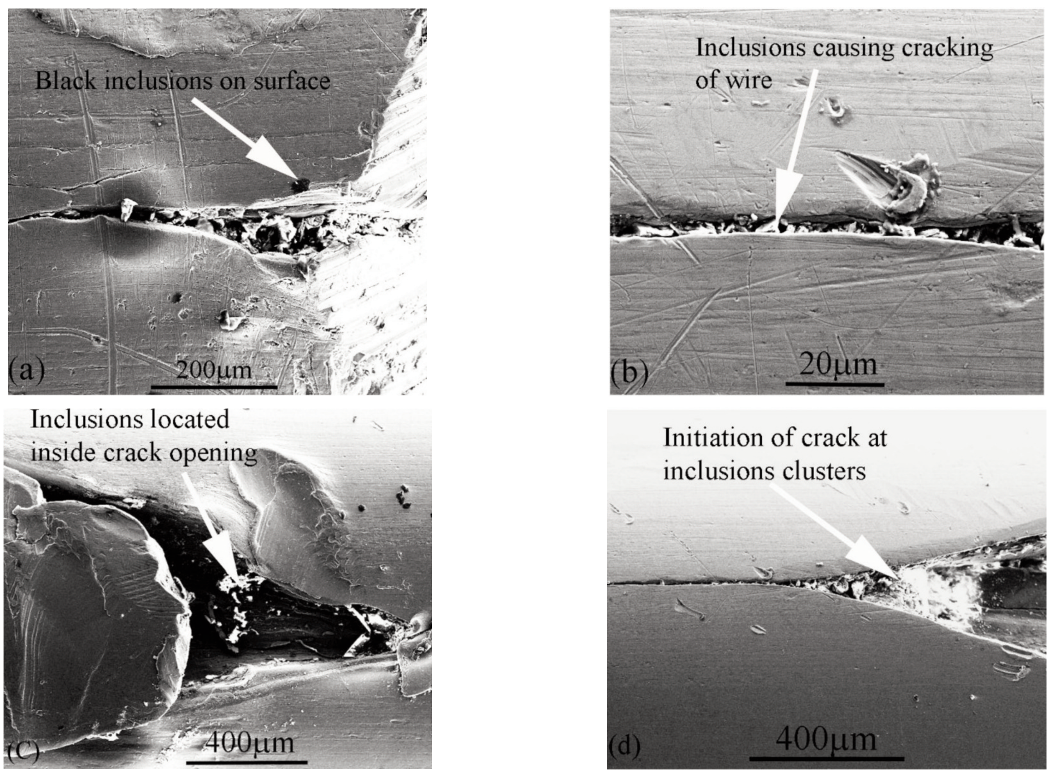

Figure 3. *SEM (SEI) images of as fractured EC grade Al wires without polishing*

CC BY SA

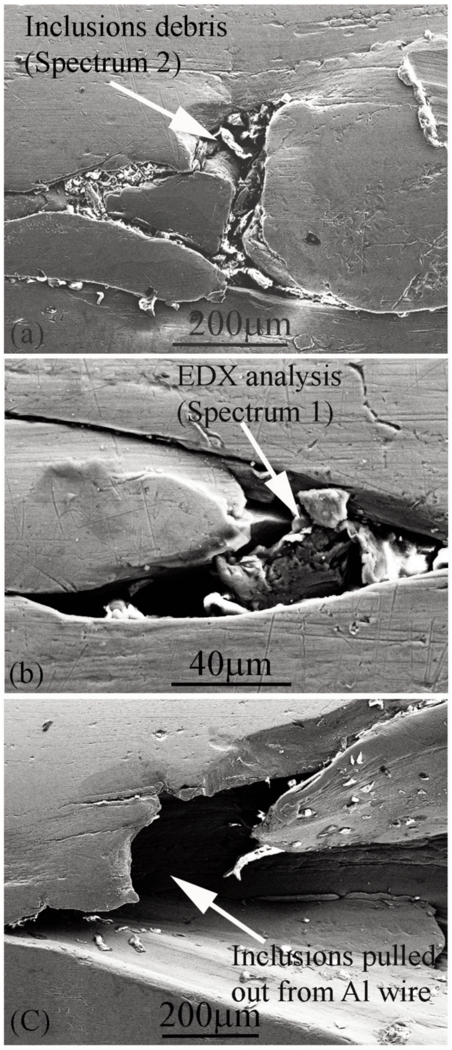

Figure 4. *SEM (SEI) images of inclusions and fractured end of Al wires*

particles in the vicinity of inclusions. Moreover, such inclusions may form clusters which are composed of several other solid phases as revealed during thermodynamic analysis. In addition to Al_2O_3 particles, inclusions composed of MgO could also be formed during boron treatment process that are detected during EDX analyses, as shown in Figure 5b.

4.2.2 Mapping of Elements

The distribution of elements in the inclusions and aluminum matrix were further studied by the EDX mapping. Mapping of the area shown in Figure 6 revealed aluminum (Figure 6a), little white spots representing carbon (Figure 6b), reasonably large white spot of Mg (Figure 6c) and uniformly distributed Oxygen (Figure 6d) in the aluminum matrix. It is evident that the inclusions containing area is rich in carbon, Magnesium and Oxygen.

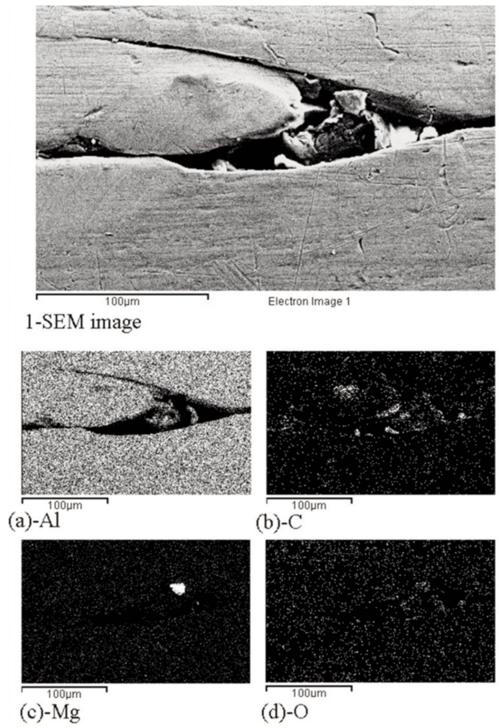

Figure 6. *SEM (Mapping) of elements present in the aluminum matrix*

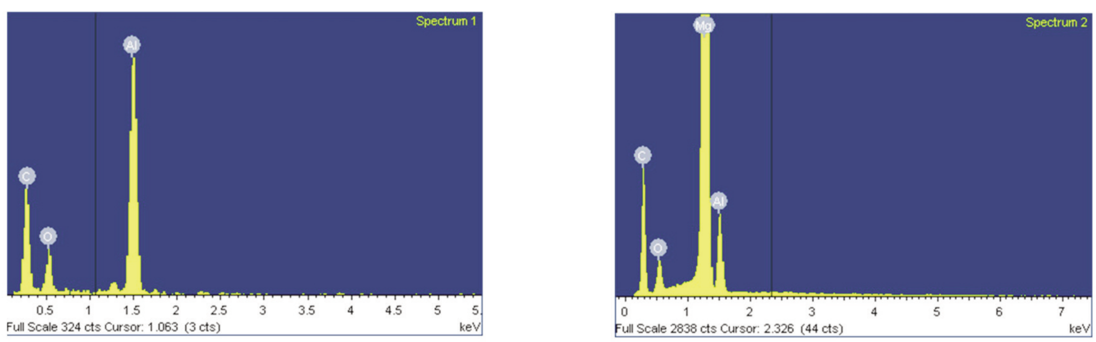

(a) (b)

Figure 5. *EDX analyses of inclusions in aluminum matrix*

4.3 Polished Samples Analysis

Selected portions of the fractured aluminum wires were sectioned and mounted in Bakelite for easy handling. The samples were then mechanically polished using SiC emery papers of 300, 600, 1200 grit and water as a lubricant. Final polishing was carried on 9, 6, 3, 1 µm diamond paste and then finally on OP-S colloidal silica suspension for 3 minutes each until scratch free surfaces were produced. The polished samples were analyzed under SEM fitted with EDX detector. The SEM (SEI) images are given in Figures 7 and 8. Inclusions of Al, Si and O in the range of approximately 1 µm to 5 µm (see Figure 7d) can be seen in the aluminum matrix. A large number of small inclusions but in cluster form can also be observed in Al matrix (Figure 7d). Black spots in Figures 7b, 7c and 7d are cavities which might have been created due to pulling out of hard inclusions (borides, carbides and nitrides) during samples preparation for SEM analysis.

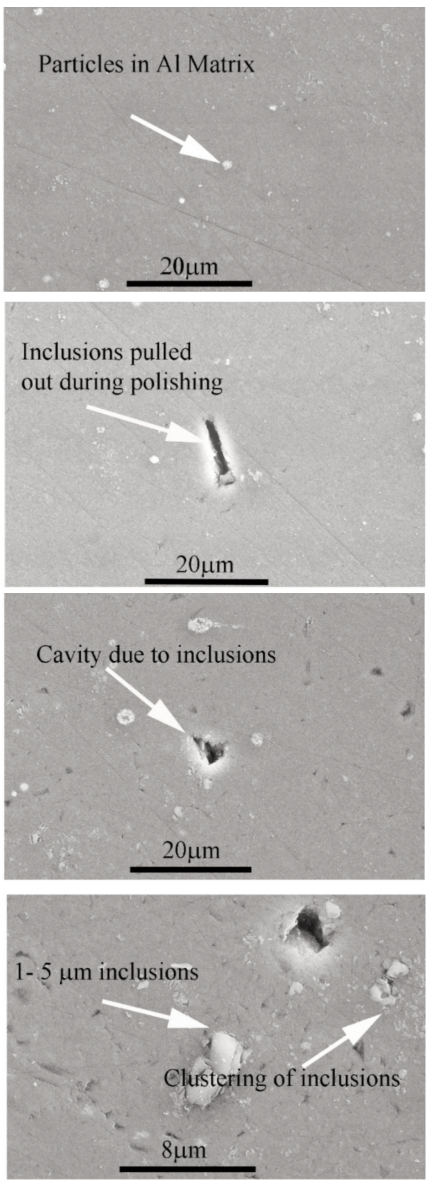

Figure 7. *SEM (SEI) of polished samples containing inclusions*

5. Findings of Failure Analysis

The SEM (SEI) image of the fractured end of a broken wire is shown in Figure 8b. This type of failure is of ductile nature which may be due to the presence of inclusions. These act as stress raiser points during wire drawing or/and another mechanical loading condition in process. At the interface between inclusions and Al–matrix, a triaxial state of stress may have been developed due to stress concentration at inclusion points. As a result, under mechanical loading, the stress level might have risen to the fracture strength of the inclusions at the interface between inclusions and Al–matrix. This had led to the broken inclusions. Another phenomenon might be the inclusions were pulled out of the Al–matrix due to less bonding strength at the interface. These broken inclusions led to the development of micro-voids at the interface, which then coalesced to produce the final ductile fracture. This hypothesis of indication of ductile fracture is further strengthened after observing the fractured surfaces, as shown in Figures 2 and 4 as these were reasonably deformed. The polished surface of the EC grade Al wire as shown in Figure 8a. A large number of small cavities as observed on the polished surface are due to the inclusions present in the alloy.

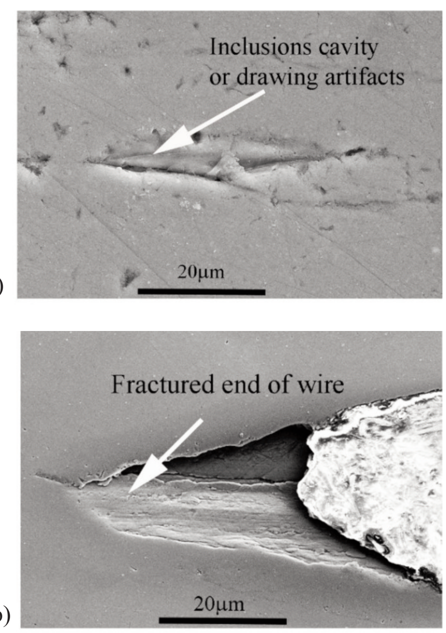

Figure 8. *SEM (SEI) of polished fractured end of wire*

6. Conclusion

In this work, failure analysis of EC grade aluminum wires was carried out which had undergone failure during wire drawing process. The preliminary investigation was carried out using SEM and EDX. The analysis of fractured Al–wire pieces revealed the presence of inclusions in the crack openings either in the form of deformed elongated or debris of oxides. This might have been the primary cause of the ductile failure of these wires during wire drawing process. The possible types of inclusions identified with EDX were Al_2O_3, Al_3C_4 (Al-Carbides), refractory bricks elements (Al, Mg, Si and O). Thermodynamic analysis using FactSage also predicted the formation of Al_2O_3 and Ca-aluminates in the molten aluminum. The oxides of aluminum (Al_2O_3) could come from alumina used in the electrolytic cells. It can also be generated by the reaction of air with melt during stirring and pouring of metal, and by the oxidation of refractory materials. Aluminum carbides form due to the presence of carbon or graphite particles in melt which are possibly coming from electrolysis process. These particles are of the size in the range 0.1 µm to 5 µm and are present mostly with oxides or borides. During this analysis, boride particles were not identified which may be fine enough to be detected with this microscope and may need to be analyzed at higher magnification. The presence of Si in the inclusions give the indication of SiO_2 or other silicates, as predicted by the thermodynamic analysis. It is recommended to use ceramic foam filters to isolate inclusions from molten aluminum. Last but not the least, improvements in melt quality will minimize the failure of EC grade aluminum wires.

References

[1] G.G. Gauthier, J. Inst. Met., 59 (1936) 129-150.

[2] W.A. Dean, Aluminum, 1 (1967) 174.

[3] W.C. Setzer, G.W. Boone, Light Metals 1992, (1991) 837-844.

[4] P.S. Cooper, M.A. Kearns, Aluminium Alloys: Their Physical and Mechanical Properties, Pts 1-3, 217 (1996) 141-146.

[5] R. Cook, M.A. Kearns, P.S. Cooper, Light Metals 1997, (1997) 809-814.

[6] S. Karabay, I. Uzman, Journal of Materials Processing Technology, 160 (2005) 174-182.

[7] S. Karabay, I. Uzman, Materials and Manufacturing Processes, 20 (2005) 231-243.

[8] G.Q. Wang, S.H. Liu, C.M. Li, Q. Gao, Transactions of Nonferrous Metals Society of China, 12 (2002) 1112-1116.

[9] A. Khaliq, M.A. Rhamdhani, G.A. Brooks, J. Grandfield, Metallurgical and Materials Transactions B: Process Metallurgy and Materials Processing Science, 47 (2016) 595-607.

[10] A. Khaliq, M.A. Rhamdhani, G.A. Brooks, J. Grandfield, Canadian Metallurgical Quarterly, 55 (2016) 161-172.

[11] W. Stiller, T. Ingenlath, Aluminium (English Edition), 60 (1984).

[12] A. Khaliq, M.A. Rhamdhani, G.A. Brooks, J.F. Grandfield, Metallurgical and Materials Transactions B: Process Metallurgy and Materials Processing Science, 45 (2014) 769-783.

[13] A. Khaliq, M.A. Rhamdhani, G.A. Brooks, J. Grandfield, TMS Light Metals, 2014, pp. 963-968.

[14] A. Khaliq, M.A. Rhamdhani, G.A. Brooks, J. Grandfield, Metallurgical and Materials Transactions B: Process Metallurgy and Materials Processing Science, 45 (2014) 784-794.

[15] A. Khaliq, M.A. Rhamdhani, G.A. Brooks, J. Grandfield, J. Mitchell, D. Cameron, EMC (European Metallurgical Conference) Dusseldorf, Germany, 2011, pp. 825-838.

[16] A. Khaliq, M.A. Rhamdhani, G.A. Brooks, J. Grandfield, TMS 2011, San Diego, CA, 2011, pp. 751-756.

[17] A. Khaliq, M.A. Rhamdhani, G. Brooks, J. Grandfield, High temperature processing symposium (HTPS), Swinburne Univeristy of Technology, Melbourne, 2011.

[18] M.A. Dewan, M.A. Rhamdhani, J.B. Mitchell, C.J. Davidson, G.A. Brooks, M. Easton, J.F. Grandfield, 2011, pp. 149-160.

[19] J. Grandfield, A. Khaliq, M.A. Rhamdhani, M. Dewan, M. Easton, L. Sweet, C. Davidson, J. Mitchell, G. Brooks, 10th Australasian Aluminium Smelting Technology Conference, Tasmania, Australia, 2011.

[20] C.K. Grjotheim, M. Malinovsky, K.Matiasovsky, J. Thonstad, Aluminium Electrolysis: Fundamentals of the Hall Heroult Process, 2nd ed., Aluminium-Verlag GmbH, D-4000 Dusseldorf, Germany, 1982.

[21] C.J. Simensen, C. Berg, Aluminium Dusseldorf, 56 (1980) 335-340.

[22] C.J. Simensen, Metallurgical Transactions B-Process Metallurgy, 12 (1981) 733-743.

[23] C.J. Simensen, Metallurgical Transactions B-Process Metallurgy, 13 (1982) 31-34.

[24] C.J. Simensen, Zeitschrift Fur Metallkunde, 84 (1993) 730-733.

[25] L. Kirkpatrick, Aluminum Electrical Conductor Handbook, The Aluminum Association, 1989.

[26] A.T. Ertürk, E.A. Güven, S. Karabay, Transactions of the Indian Institute of Metals, 68 (2015) 535-541.

[27] S. Karabay, Materials & Design, 29 (2008) 1364-1375.

[28] S. Karabay, E.A. Güven, A.T. Ertürk, Engineering Failure Analysis, 31 (2013) 153-160.

[29] S. Karabay, E.A. Güven, A.T. Ertürk, Materiali in Tehnologije, 47 (2013) 119-124.

[30] A.T. Erturk, E.A. Guven, S. Karabay, Acta Physica Polonica A, 127 (2015) 1292-1294.

[31] T.A. Engh, Principles of Metal Refining, Oxford University Press, 1992.

CC BY SA